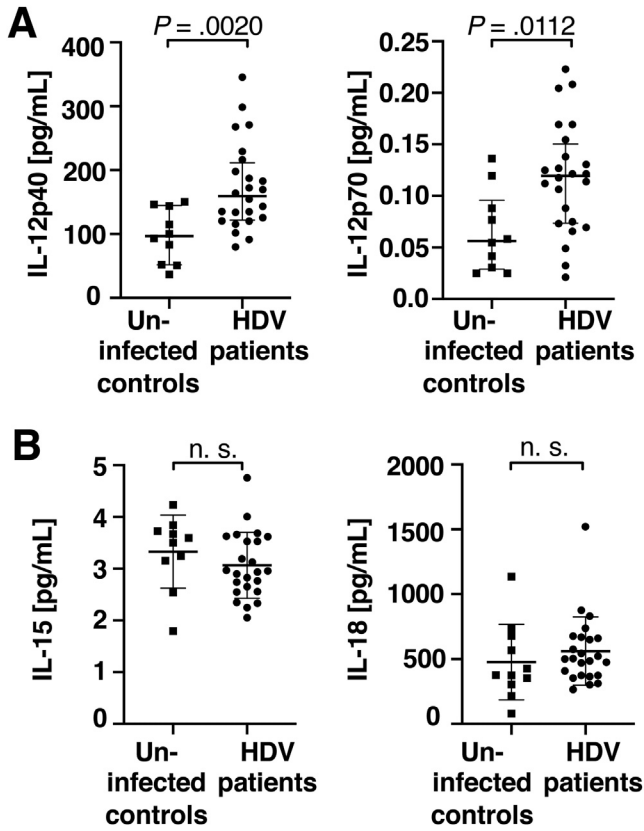
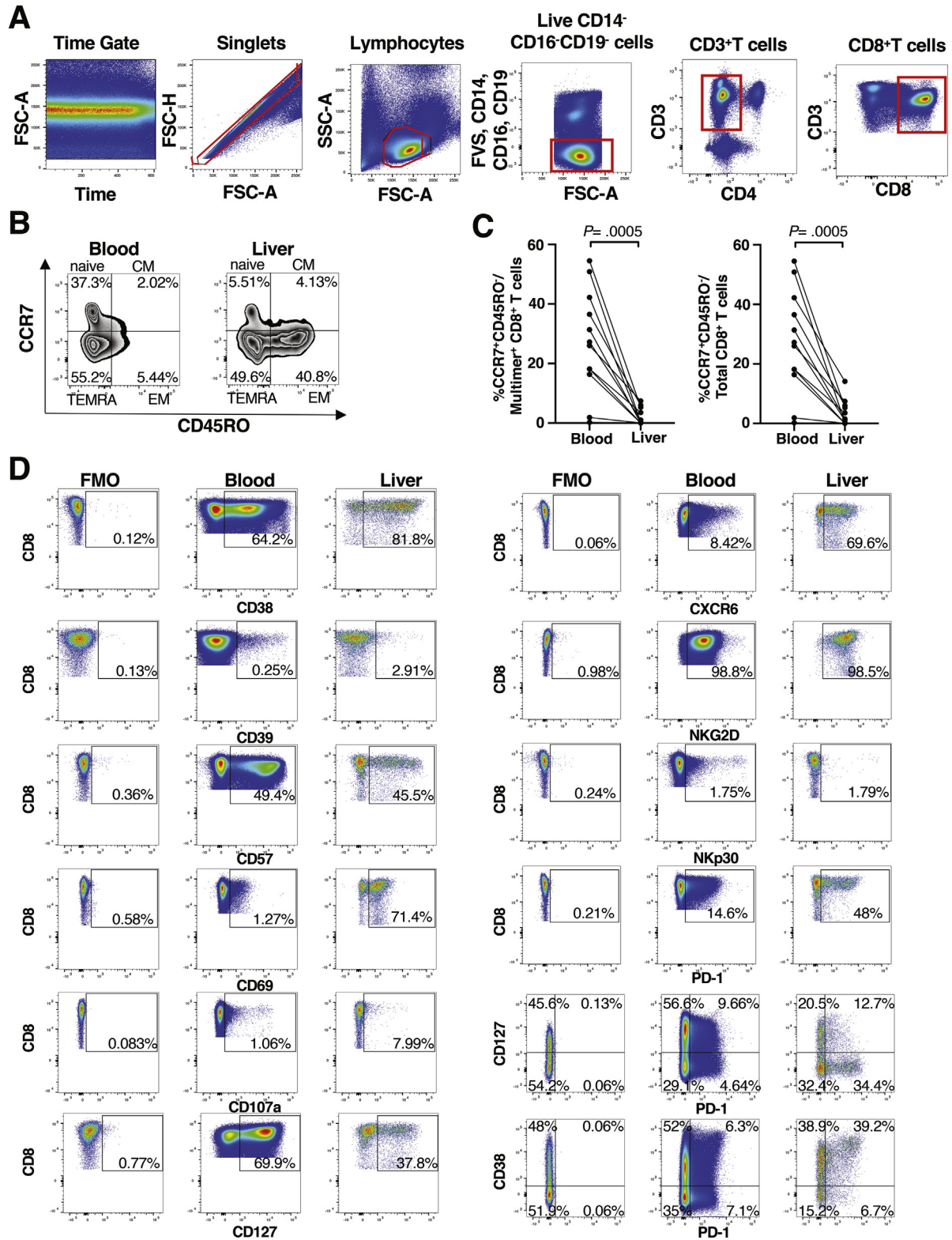


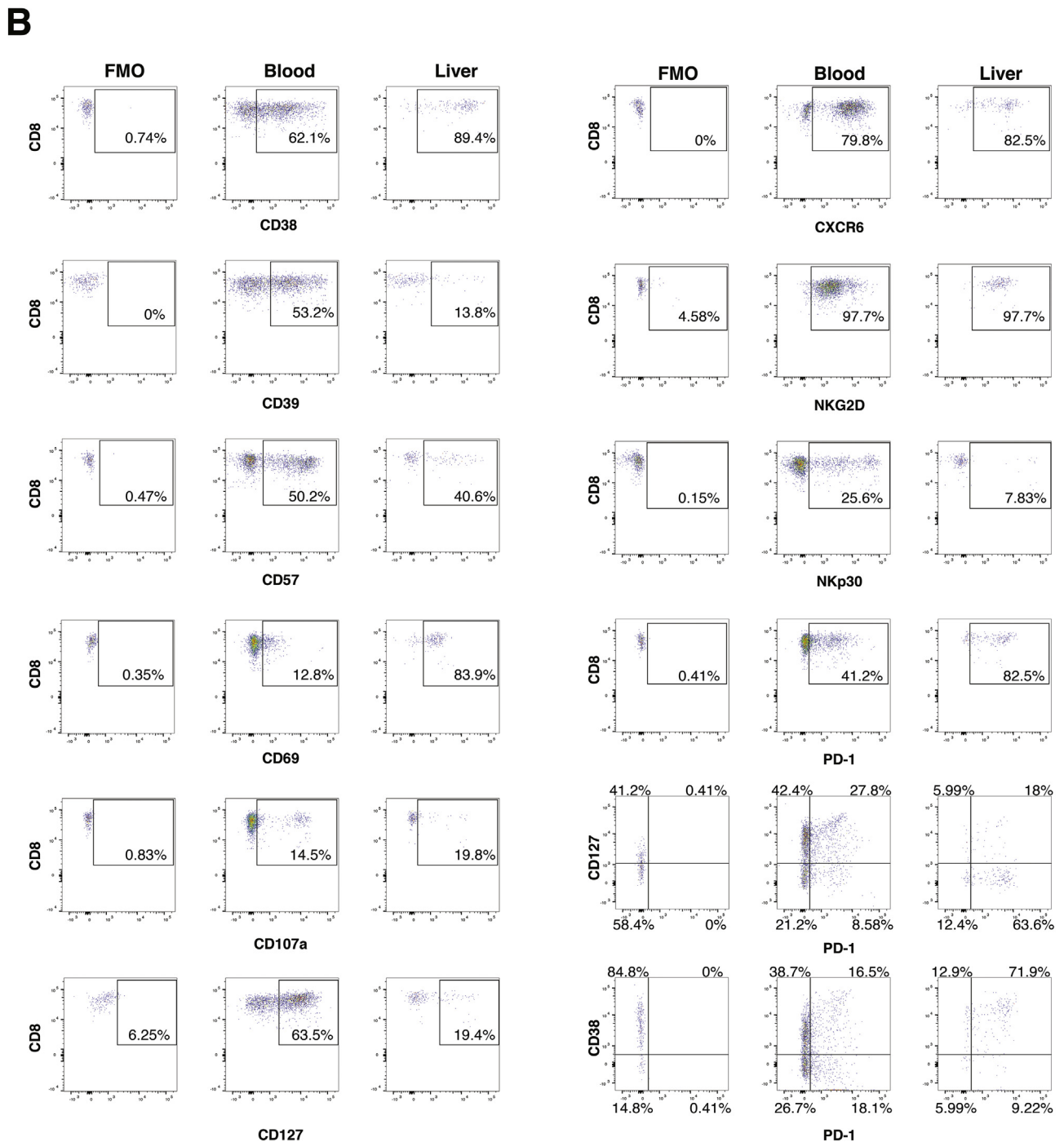
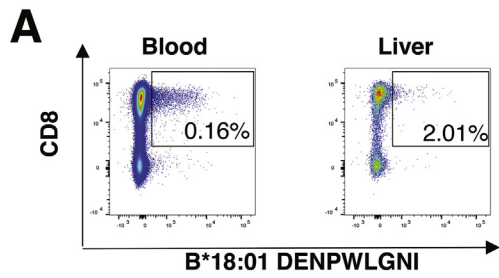
Supplementary Figure 1. Gating strategy to characterize innate immune cells. (A) The gating strategy included a time gate, followed by gating on singlets and lymphocytes, exclusion of dead, CD14⁺, CD16⁺, and CD19⁺ cells, and gating on CD3⁺ or CD3⁻ cells. The respective gates are shown in red. (B) After gating on CD3⁺ cells, MAIT cells were identified as TCRVa7.2⁺CD161⁺ cells. The frequency of HLA-DR⁺ and CD107a⁺ MAIT cells was determined in blood and liver based on the respective fluorescence-minus-one control (FMO). (C) NK cells were identified as CD3⁻CD56⁺ cells. The frequency of HLA-DR⁺ and CD107a⁺ NK cells was determined in blood and liver based on the respective fluorescence-minus-one control (FMO). FSC-A, forward scatter area; FSC-H, forward scatter height; SSC-A, side scatter area; FVS: fixable viability stain.



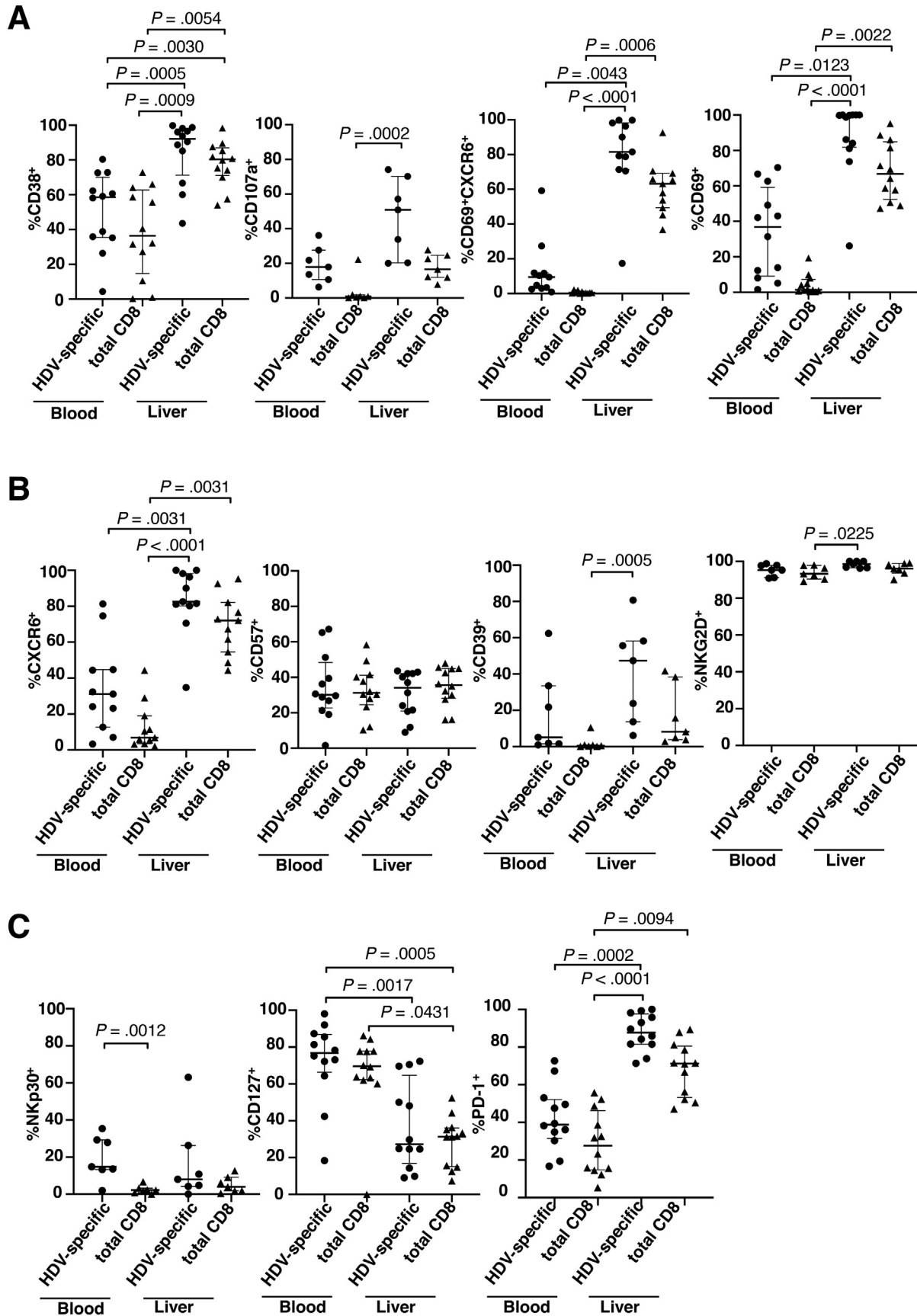
Supplementary Figure 2. Plasma levels of MAIT and NK cell-stimulating cytokines in patients infected with HDV and uninfected controls. Plasma levels of (A) the two IL12 subunits and (B) IL15 and IL18 in the plasma of uninfected controls and patients infected with HDV. Median and interquartile range with Mann-Whitney U tests are shown. n.s., not significant.



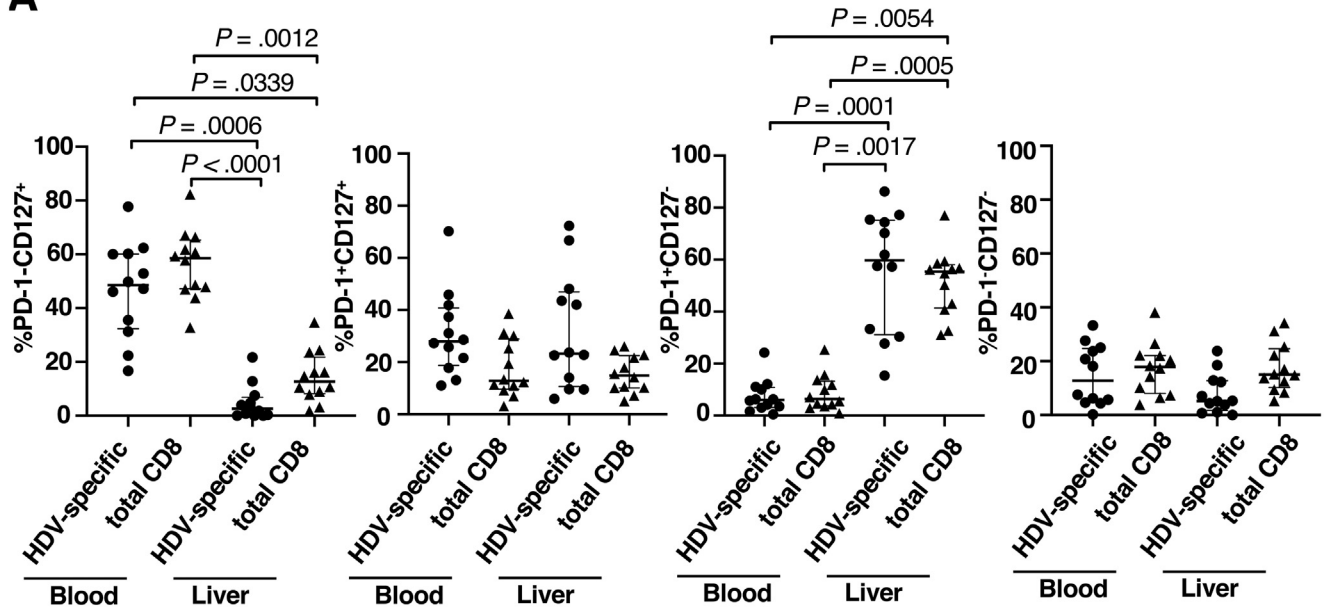
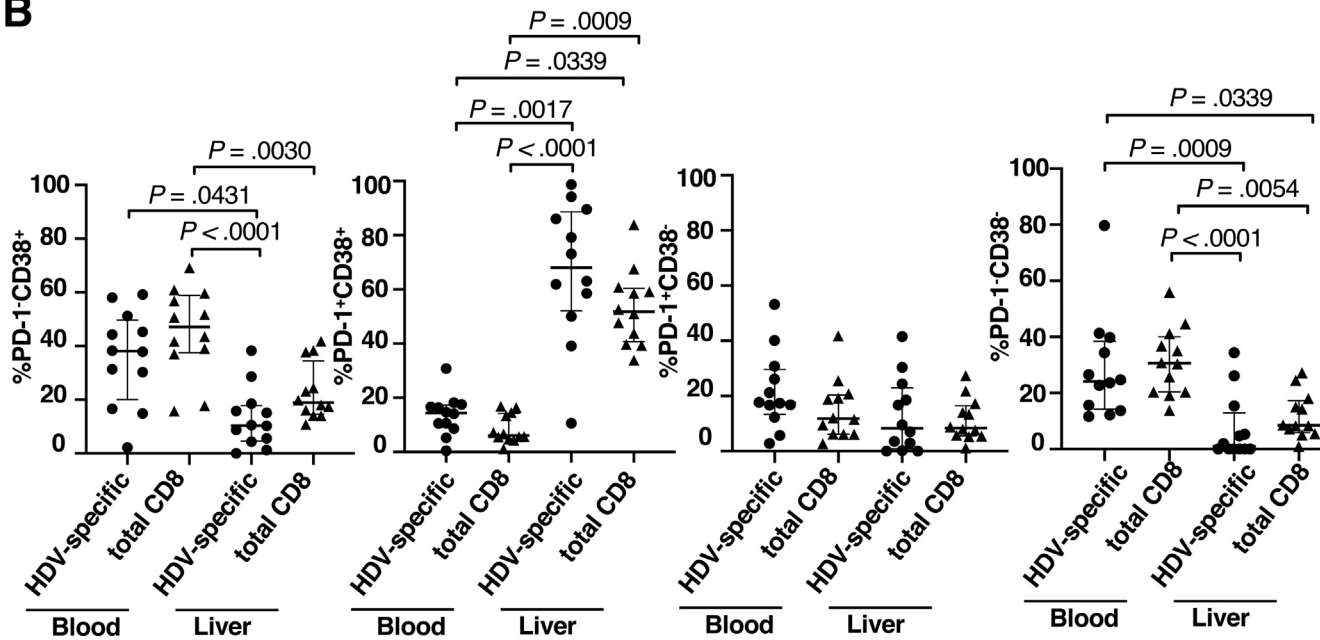
Supplementary Figure 3. Gating strategy to characterize total CD8⁺ T cells. (A) CD8⁺ T cells were identified by sequentially setting a time gate, followed by gating on singlets and lymphocytes, exclusion of dead, CD14⁺, CD16⁺, and CD19⁺ cells, gating on CD3⁺CD4⁻ T cells, and gating on CD8⁺ T cells. The respective gates are shown in red. (B) Gating of naïve, central memory (CM), effector memory (EM), and TEMRA cells within the CD8⁺ T-cell population in blood and liver. (C) Naïve (CCR7⁺CD45RO⁻) cells among HDV-specific and total CD8⁺ T cells in blood and liver. (D) Identification of blood and liver CD8⁺ T cells that express the indicated cell surface markers. The gates were set based on the respective fluorescence-minus-one (FMO) control.



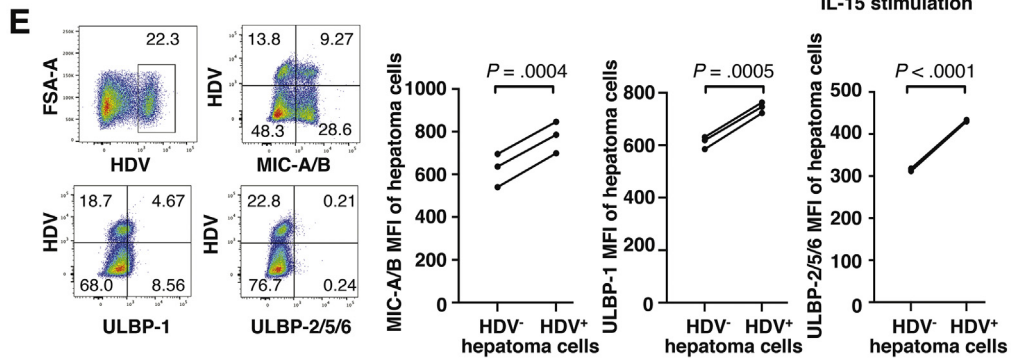
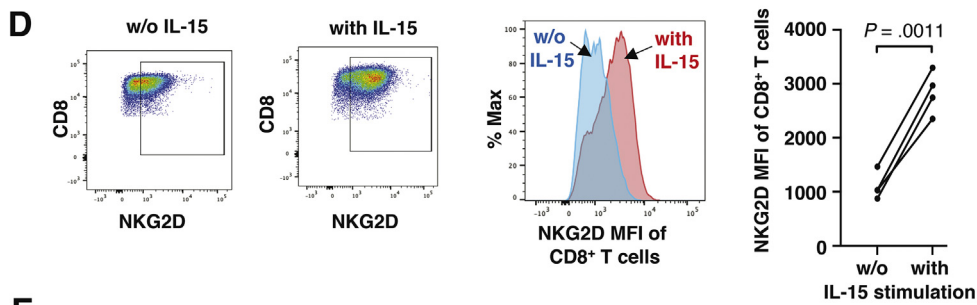
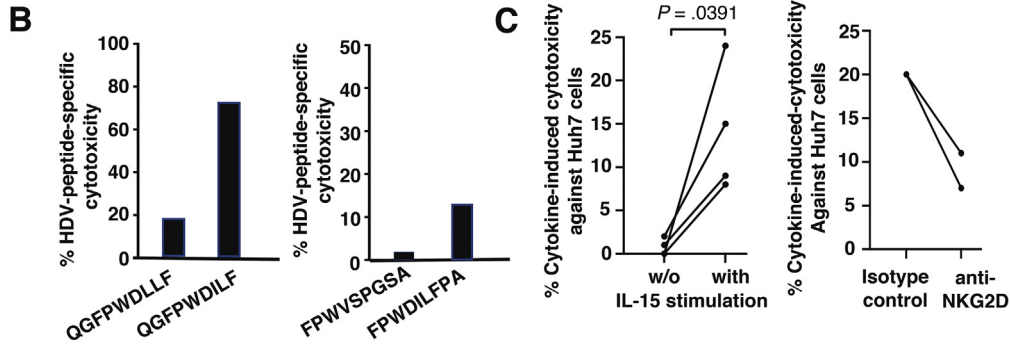
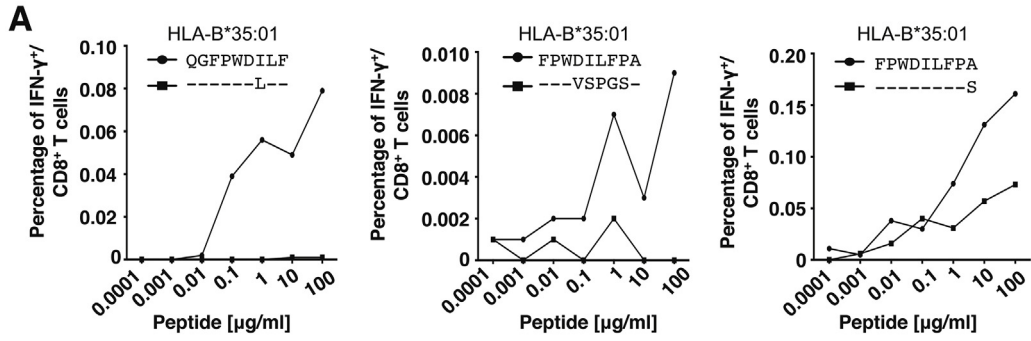
Supplementary Figure 4. Gating strategy to characterize HDV-specific CD8⁺ T cells. (A) Identification of HDV-specific cells within the CD8⁺ T-cell population in blood and liver. (B) Identification of blood and liver HDV-specific CD8⁺ T cells that express the indicated cell surface markers. The gates were set based on the respective fluorescence-minus-one (FMO) control.



Supplementary Figure 5. Phenotype of HDV-specific and total CD8⁺ T cells in blood and liver. (A) Frequency of CD38⁺, CD107a⁺, CD69⁺CXCR6⁺, and CD69⁺ HDV-specific and total CD8⁺ T cells in blood and liver. (B) Frequency of CXCR6⁺, CD57⁺, CD39⁺, NKG2D⁺ HDV-specific, and total CD8⁺ T cells in blood and liver. (C) Frequency of NKp30⁺, CD127⁺, PD-1⁺ HDV-specific, and total CD8⁺ T cells in blood and liver. The data correspond to the radar plot shown in Figure 4.

A**B**

Supplementary Figure 6. Frequency of HDV-specific and total CD8⁺ T-cell subsets that express combinations of CD127 and PD-1 or PD-1 and CD38. HDV-specific and total CD8⁺ T-cell subsets in blood and liver are analyzed based on (A) PD-1/CD127 and (B) PD-1/CD38 expression. The data correspond to the radar plot in [Figure 4](#).



Supplementary Figure 7. Effector function of CD8⁺ T-cells after HDV-specific, TCR-mediated, and after cytokine-mediated, TCR-independent activation. (A and B) HDV-specific, TCR-mediated CD8⁺ T-cell effector functions: HDV-specific T-cell lines were generated from PBMCs of patients 23, 10, and 11 with chronic HDV infection. The generated T-cell lines were restimulated with dose titrations of epitopes with the prototype HDV genotype 1 sequence or the autologous sequence (representing the HDV sequence in patient sera) and assessed for (A) IFN- γ production by intracellular cytokine staining (B) or for cytotoxicity against peptide-pulsed HLA-B*3501⁺ target cells. The prototype peptide sequence is shown above the panel, and the autologous sequence is aligned to it. The HLA-restriction of the respective prototype peptide is indicated above each panel. (C) Cytokine-induced, TCR-independent CD8⁺ T-cell cytotoxicity: CD56-depleted, IL15-stimulated or not stimulated PBMCs from HDV-uninfected blood donors were tested for cytotoxicity against the hepatoma cell line Huh7. The donors did not share any HLA class I allele with Huh7 cells. The cytotoxicity assay with CD56⁺ cell-depleted, IL15-stimulated PBMCs was repeated in the presence of an anti-NKG2D or isotype control antibody. (D) CD56⁺ cell-depleted, IL15-stimulated or not stimulated PBMCs were assessed for NKG2D expression. The dot plots are gated on CD8⁺ T cells. (E) The HDV-producing hepatoma cell line Huh7-END was assessed for intracellular HDV antigen expression and for cell surface expression of NKG2D ligands (MIC-A/B, ULBP-1, and ULBP-2/5/6). To compare the frequency of MIC-A/B-, ULBP-1- or ULBP-2/5/6-expressing cells in the HDV⁺ and in the HDV- cell population, the number in the upper right quadrant of the respective dot plot is to be divided by the sum of the numbers in the upper right and upper left quadrants and then compared to the number in the lower right quadrant divided by the sum of the numbers in the lower right and lower left quadrants. Statistics: paired *t* tests.

Supplementary Table 1.Antibodies Used for Staining of Mononuclear Cells

Specificity	Fluorochrome	Clone	Vendor	Antibody panel	Dilution
Viability	FVS 510	N/A	BD Biosciences	1, 2, 3	1:333
CD14	V500	M5E2	BD Biosciences	1, 2, 3	1:25
CD14	PE-Cy7	M5E2	BD Biosciences	1	1:50
CD16	V500	3G8	BD Biosciences	2, 3	1:800
CD16	PE-Cy5	3G8	BD Biosciences	1	1:800
CD19	V500	HIB19	BD Biosciences	1, 2, 3	1:100
CD3	APC-Cy7	SK7	BD Biosciences	2, 3	1:20
CD3	Alexa Fluor 700	SK7	BioLegend	1	1:100
CD4	BUV 496	SK3	BD Biosciences	3	1:50
CD4	eF450	SK3	eBiosciences	2	1:50
CD8	PerCP	SK1	BioLegend	2	1:100
CD8	BUV 805	SK1	BD Biosciences	3	1:200
CCR7	BV785	G043H7	BioLegend	2, 3	1:25
CD45RO	FITC	UCHL1	BioLegend	2	1:25
CD45RO	BUV 395	UCHL1	BD Biosciences	3	1:50
CD127	PE-Cy7	A019D5	BioLegend	2, 3	1:100
CD38	BV711	HIT2	BioLegend	2	1:20
CD38	APC-R700	HIT2	BD Biosciences	3	1:100
CD39	BUV737	TU66	BD Biosciences	3	1:400
CD56	PE-Dazzle	HCD56	BioLegend	1	1:200
CD57	eF450	TB01	eBiosciences	3	1:50
CD57	Alexa Fluor 647	HNK-1	BioLegend	2	1:50
CD69	BV605	FN50	BioLegend	1	1:200
CD69	APC-Cy7	FN50	BioLegend	1	1:100
CD161	BV421	DX12	BD Biosciences	1	1:10
CXCR6	PE-Dazzle	K041E5	BioLegend	2	1:100
CXCR6	BUV563	13B 1E5	BD Biosciences	3	1:14
PD-1	BV650	EH12.2H7	BioLegend	2, 3	1:50
NKp30	BB700	P30-15	BD Biosciences	3	1:100
NKG2D	BV711	1D11	BD Biosciences	3	1:50
TCR Va7.2	FITC	3C10	BioLegend	1	1:50
TRAIL	APC	RIK-2	BD Biosciences	1	1:50
HLA-DR	BV711	G46-6	BD Biosciences	1	1:50
CD107a	PE	H4A3	BD Biosciences	1	1:50
CD107a	PE-Cy5	H4A3	BD Biosciences	3	1:10

APC, allophycocyanin; BB, BD Horizon Brilliant Blue; BUV, BD Horizon Brilliant Ultraviolet; BV, BD Horizon Brilliant Violet; Cy7, cyanine dye 7; FITC, fluorescein isothiocyanate; FVS, Fixable Viability Stain; PE, phycoerythrin; TRAIL, tumor necrosis factor-related apoptosis-inducing ligand.